

Basic Research for Electroretinogram Moving the Center of the Multifocal Hexagonal Stimulus Array

Naoto Suzuki

Abstract—Many ophthalmologists can examine declines in visual sensitivity at arbitrary points on the retina using a precise perimetry device with a fundus camera function. However, the retinal layer causing the decline in visual sensitivity cannot be identified by this method. We studied an electroretinogram (ERG) function that can move the center of the multifocal hexagonal stimulus array in order to investigate cryptogenic diseases, such as macular dystrophy, acute zonal occult outer retinopathy, and multiple evanescent white dot syndrome. An electroretinographic optical system, specifically a perimetric optical system, was added to an experimental device carrying the same optical system as a fundus camera. We also added an infrared camera, a cold mirror, a halogen lamp, and a monitor. The software was generated to show the multifocal hexagonal stimulus array on the monitor using C++Builder XE8 and to move the center of the array up and down as well as back and forth. We used a multifunction I/O device and its design platform LabVIEW for data retrieval. The plate electrodes were used to measure electrodermal activities around the eyes. We used a multifocal hexagonal stimulus array with 37 elements in the software. The center of the multifocal hexagonal stimulus array could be adjusted to the same position as the examination target of the precise perimetry. We successfully added the moving ERG function to the experimental ophthalmologic device.

Keywords—Moving ERG, precise perimetry, retinal layers, visual sensitivity.

I. INTRODUCTION

FOR precise perimetry examination, a projected light stimulus is used to measure the patient's field of view. The examination target is projected in the visual field areas while an ophthalmologist sees the patient's fundus image directly. And the precise perimetry is used to measure the visual sensitivity in target area [1]. On the other hand, the retina consists of 10 layers as shown in Fig. 1. However, it is important to find an examination method which can perfectly identify the retinal layer causing visual sensitivity declines. The ERG displays a multifocal hexagonal stimulus array with intermittent flashes of light and is able to measure the electric potential of the reactions through contact lens or plate electrodes. The ERG is mainly used to diagnose retinitis pigmentosa. For example, the reaction electric potentials of an ERG decrease remarkably from the early stage of the disease. And the ERG reaction is undetectable by the middle stages. A patient having cone-rod dystrophy was shown to lack recordable signals for reaction after ROD and CONE ERGs [2]. Moreover, patients with juvenile retinal degeneration had concentric contractions and

lacked recordable signals to the bright flash ERG [3]. Moreover, the ERG waveforms shown in Fig. 2 are related to the retinal layer causing a decline in the visual sensitivity [2]. That is to say, four different waveforms reflect the decline in the visual sensitivity of separate layers of the retina: the wave represents signals from the layer of rods and cones; the b wave, from the inner nuclear layer; the c wave, from the retinal pigment epithelium; and the photopic negative response, from the ganglion cell layer [2], [4], [5]. However, the conventional ERG cannot be used to move the position of the multifocal hexagonal stimulus array, and so it can only measure the ERG waveforms at the predetermined positions as shown in Fig. 3 (a). The layer causing a decline in the visual sensitivity can be detected if the center of the multifocal hexagonal stimulus array of the ERG is in the same position as the examination target, as shown in Fig. 3 (b).

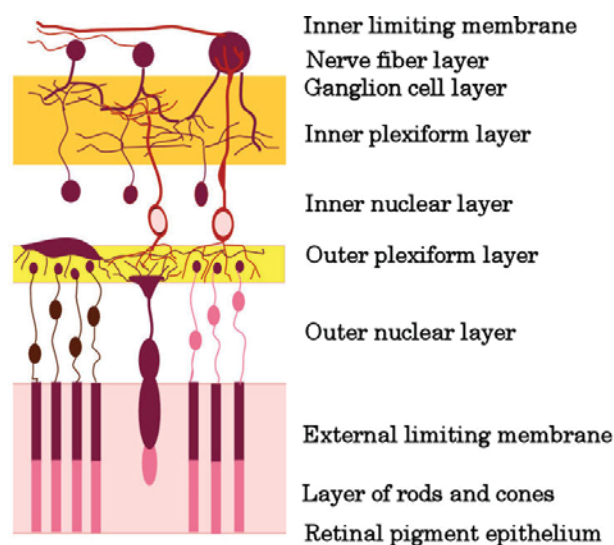


Fig. 1 Ten-layer retinal structure

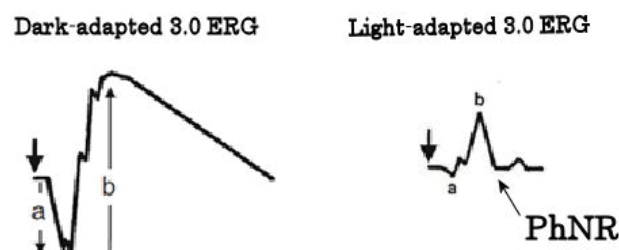


Fig. 2 Waveforms of ERG

N. Suzuki is with National Institute of Technology, Numazu College, Numazu, Shizuoka, 4108501, Japan and is financially supported by Terumo Foundation for Life Sciences and Arts, Ashigarakamigun, Kanagawa, 2590151, Japan (e-mail: n-suzuki@numazu-ct.ac.jp).

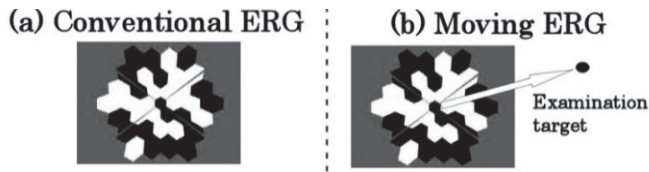


Fig. 3 Conventional ERG and moving ERG

ERGs are useful in trying to find causes for the decline in visual sensitivity. And it is desirable to find out if a disorder involves the retinal pigment epithelium, the photoreceptor layer, or the ganglion cell layer. We will now review the pathogenic mechanisms of cryptogenic diseases such as macular dystrophy, acute zonal occult outer retinopathy (AZOOR), and multiple evanescent white dot syndrome (MEWDS). Macular dystrophy is a disease of both eyes and is a general term for functional disorders of the macula lutea including Stargardt disease [6], [7], occult macular dystrophy [8], vitelliform macular dystrophy [9], and cone-rod dystrophy. When patients with macular dystrophy get a full-field ERG, the function of the CONE and the ROD areas is normal, but the function of the macula lutea is abnormal. AZOOR is a disease that also causes an acute functional disorder to an outer layer of the retina [10]. It is seen in young women and tends to be accompanied by photopsia. The disease is accompanied by a rapid visual loss and visual field defect. The fundus of the eye is almost normal, and ERG shows an unusual result and is effective for diagnosis. MEWDS affects young women, causing acute visual loss and a reduced visual field [11]. In addition, the Mariotte blind spot is enlarged. When the symptoms of the disease appear, white dots are scattered from a deep layer of the retina to the retinal pigment epithelium. The white dots disappear in about a few days or weeks after that. The focal ERG results show an amplitude decline in the areas of the abnormal visual field [12]. Suzuki et al. developed the precise perimetry equipment; they tested it as a glaucoma diagnostic support system and proved its usefulness [13]. This equipment acts both as a fundus camera and a perimeter. Ophthalmologists can measure the visual sensitivity while examining the fundus images photographed beforehand. Moreover, the equipment processes the fundus images and extracts some features like the intravenous lines below disc rim. Additionally, the equipment can measure the eye movement using the extracted image. On the other hand, Suzuki et al. [13] also developed an experimental device with the same optical system contained in a fundus camera as shown in Fig. 4.

Researchers tested the device on an automatic method to distinguish the small hemorrhages, the hard exudates, and the photocoagulation marks from image artifacts. Results were positive for the automatic distinction using the color spaces [14], [15]. And, we are developing an ophthalmology examination device that displays the multifocal hexagonal stimulus arrays and the examination targets on a monitor as shown in Fig. 5.

The device can perform ERGs and precise perimetry and serve as a fundus camera. Moreover, the conventional ERG cannot be used to move the multifocal hexagonal stimulus array

as shown in Fig. 3 (a), and therefore, patients can only be examined at predetermined positions, meaning the affected area can only be measured if it matches the predetermined area. Our tested device uses an ERG function that allows for adjustments to the center of the multifocal hexagonal stimulus array. The moving ERG makes the central position of the multifocal hexagonal stimulus array coincide with the position of the examination target in the precise perimetry. And it measures ERG at the desired target areas as shown in Fig. 3 (a). As a consequence, the declines in visual sensitivity at arbitrary points on the retina can be examined using the precise perimetry device containing a fundus camera function. However, the retinal layer causing this decline in visual sensitivity cannot be identified. To investigate cryptogenic diseases, we evaluated an ERG function that can move the center of the multifocal hexagonal stimulus array.

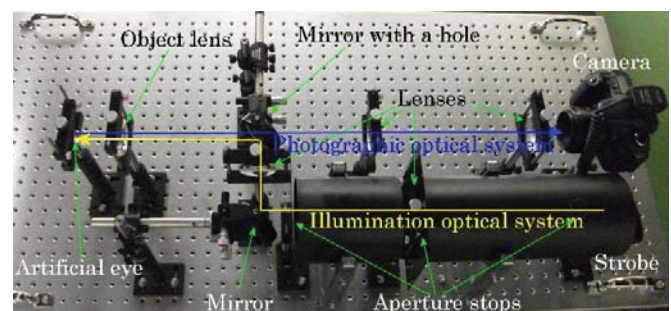


Fig. 4 Experimental devices with an optical system of the fundus camera

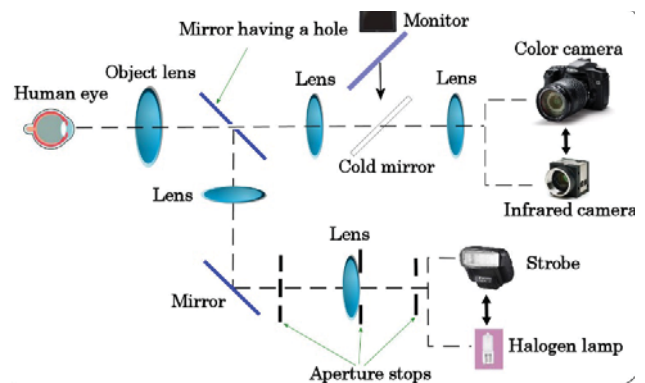


Fig. 5 Ophthalmologic examination device

II. METHODS

A. Experimental Device

As shown in Fig. 6, we constructed an experimental apparatus comprising three ophthalmologic devices: The fundus camera, an ERG, and a precise perimeter. The experimental device has illumination and photographic optical systems, separated by a mirror with a 4 mm hole. The yellow line shows the illumination optical system, and the blue line shows the photographic optical system. Moreover, our machine has a precise perimetry optical system and an electroretinographic optical system that are separated by the cold mirror. The red line shows these two optical systems. The

device consists of an infrared camera, a halogen lamp, an object lens with a 50 mm focal length, four double-convex lenses with

a 100 mm focal length, two aperture stops, a mirror, a 45° cold mirror, a monitor, and an artificial eye.

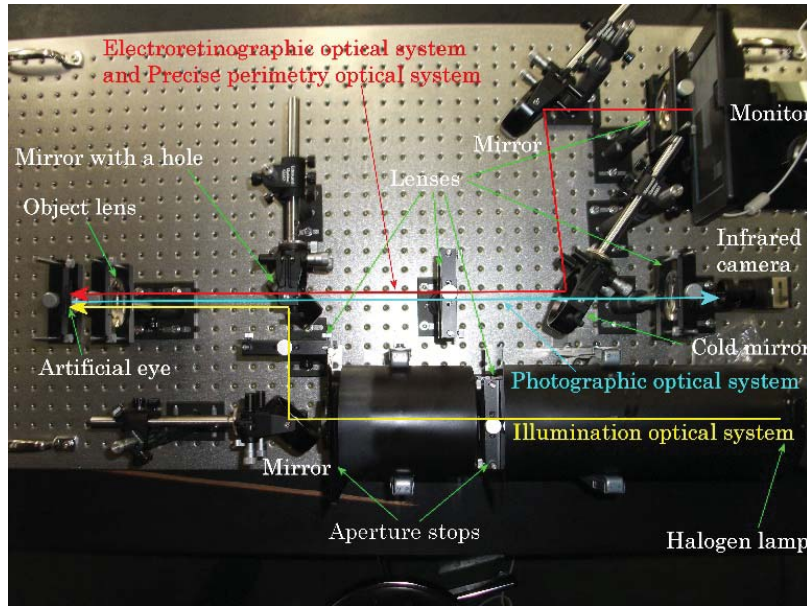


Fig. 6 Experimental device

We used an Edmund infrared camera EO-0413 with a lens of 25 mm focal length. The halogen lamp is a Philips halogen non-reflector lamp 7027 (50W, G6.35, 12V, 1CT). An 8-inch monitor shows the examination targets of the precise perimetry test and the multifocal hexagonal stimulus array of the ERG test. The monitor is an 8-inch analog RGB monitor LCD-8000V (made in Century Corp.). The display resolution is 800 x 600 pixels SVGA, and the maximum brightness is 250 cd/m². The artificial eye that we incorporated into our device is the Gullstrand artificial eye [16], which consists of a plane-convex lens, black spacer, and hemispherical cup, as shown in Fig. 7.

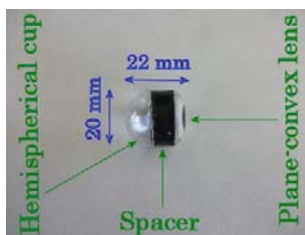


Fig. 7 Artificial eye

The plane-convex lens (made in Edmund Optics Japan) is 20 mm in diameter, 17.4 mm in back focal length, and 4.6 mm thick. The black spacer is 20 mm in outer diameter and 1 mm in thickness. The hemispherical cup has a 20 mm outer diameter and is 0.5 mm thick. The distance from the surface of the plane-convex lens to the fundus of the artificial eye is 22 mm.

B. New Electrorretinogram Software

We developed a new ERG software using Embarcadero C++Builder XE8. The software was developed to display the

multifocal hexagonal stimulus array on the monitor. This software is able to measure the x and y coordinates of the target position when a doctor clicks at a desired position on the fundus image using a mouse, as shown in Fig. 8. Our software can move the center of the array up and down as well as left and right, as shown in Fig. 9.

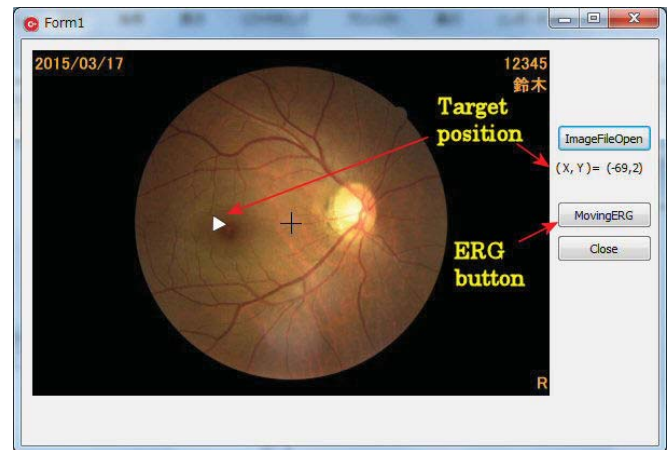


Fig. 8 ERG software

C. Electrical Measuring Equipment

We developed the equipment to measure the electrical activities of the retina. As shown in Fig. 10, we used the system design platform LabVIEW 2016, a multifunction I/O device USB-6008 (made by National Instruments), an electronic amplifier, plate electrodes, and a personal computer.

The analog input resolution of the USB-6008 device is 12 bits (differential) or 11 bits (single-ended). The maximum sample rate was 10 KS/s. The electronic amplifier comprises a

differential amplifier, a high-pass filter, and two non-inverting amplifiers. The differential amplifier is directly connected to the plate electrodes.

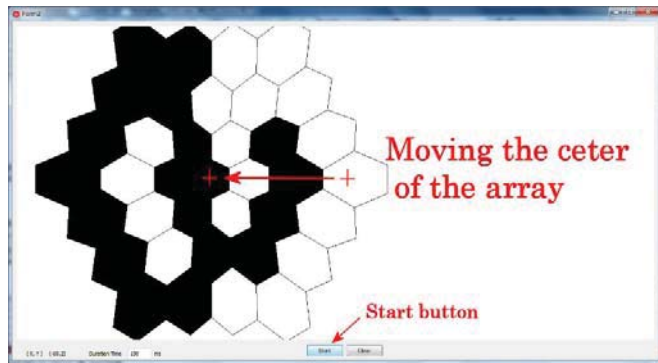


Fig. 9 Moving ERG

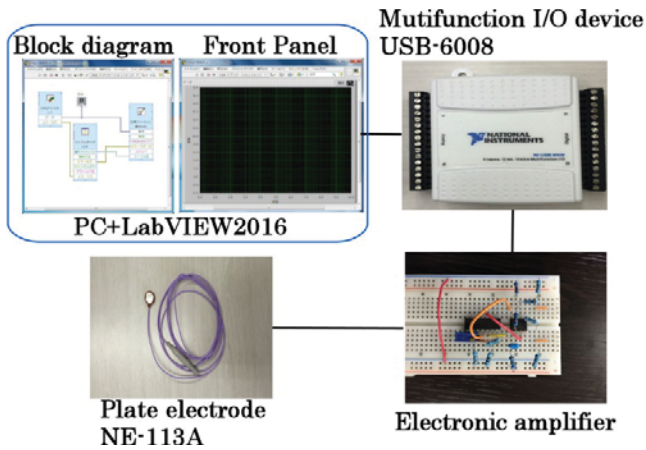


Fig. 10 Electrical measuring equipment

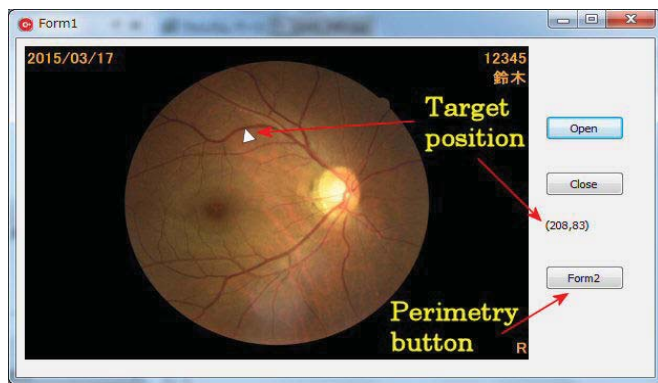


Fig. 11 Precise perimetry software

The Nihon Kohden plate electrode NE-113A was used to measure electrodermal activities around the eyes. The electrodermal activities we found were very small (such as about 10 μ V). Therefore, the gain of the differential amplifier was set at 10. The differential amplifier comprises a precision operational amplifier OP07 (made by Texas Instruments), two resistances of 100K ω \pm 1% and two resistances of 10K ω \pm 1%. In our tests, the gap between the electrodes produced waves of 10-20 Hz frequencies. So we used a resistance of 7.5 K ω and a

capacitor of 1 μ F electric capacity and made high-pass filter having a 21.2 Hz cutoff frequency. A precision picoampere current quad operational amplifier OP497 (made by Analog Devices) was used to make the two non-inverting amplifiers. The gain of the first non-inverting amplifier was set at 1001.

The non-inverting amplifier comprises a resistance of 100K ω \pm 5% and a resistance of 100 ω \pm 5%, respectively. We needed to enable the electronic amplifier to change the gain, so the second non-inverting amplifier comprised a variable resistance of 500 K ω and resistance of 10K ω \pm 5%. The gain of the non-inverting amplifier can be adjusted from 1 to 51.

D. Precise Perimetry

Fig. 11 displays a situation in which the position of the examination target is selected in the precise perimetry test. The examination target can be displayed on the same x and y coordinates in the perimetric window after an examiner clicks on the perimetry button. Fig. 12 displays the situation in which the examination target is displayed in the precise perimetry test.

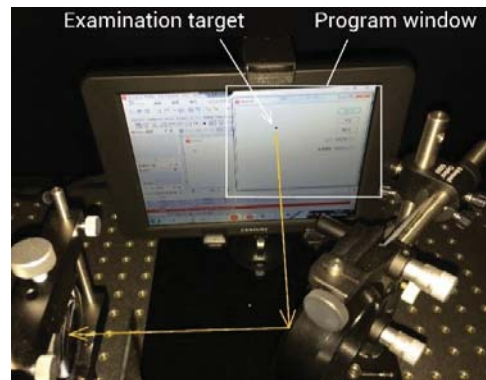


Fig. 12 The situation of precise perimetry examination

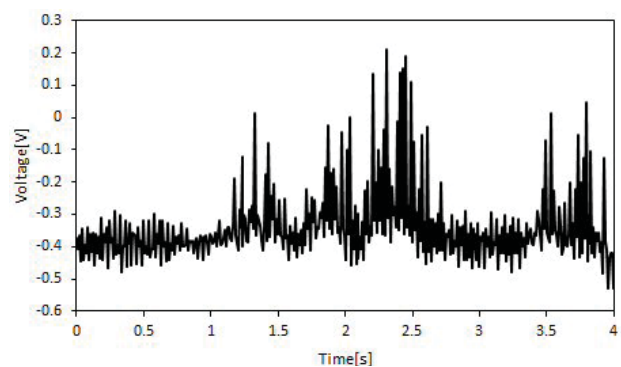


Fig. 13 Example of ERG measurement data

III. RESULTS

We used a multifocal hexagonal stimulus array with 37 elements in the software. The center of the multifocal hexagonal stimulus array could be adjusted to the same position as that of the examination target for the precise perimetry. We measured electrodermal activities around the eyes of healthy individuals aged 19-20 years. Fig. 13 presents a representative example of these electrodermal activities in healthy individuals.

IV. CONCLUSION

We successfully integrated a novel moving ERG function to our experimental ophthalmology device. And we made it possible to measure ERGs in the same positions of precise perimetry. Noises from electrodermal activity need to be reduced by repairing the electronic amplifier.

REFERENCES

- [1] E. Midea, P.P. Radin, E. Pilotto et al, "Fixation pattern and macular sensitivity in eyes with subfoveal choroidal neovascularization secondary to age-related macular generation . A microperimetry study", *Seminars in Ophthalmology*, Vol.19 Nos.1-2, 2004, pp55-61.
- [2] M.F. Marmor, A.B. Fulton, G.E. Holder et al, "ISCEV Standard for full-field clinical electroretinography (2008 update)", *Doc Ophthalmol*, Vol.118 No.1, 2009, pp69-77.
- [3] K. Kuniyoshi, H. Sakuramoto, K. Yoshitake, et al, "Longitudinal clinical course of three Japanese patients with Leber congenital amaurosis / early-onset retinal dystrophy with RDH12 mutation", *Doc Ophthalmol*, Vol.128 No.3, 2014, pp219-228.
- [4] L. Frishman, "Origin of the Electroretinogram", in *Principles And Practice of Clinical Electrophysiology of Vision*, 2nd ed, J. Heckenlively, G. Arden, N. Steven, et al, Cambridge:MIT Press, 2006, pp139-183.
- [5] A. Farkas, "Electroretinography(ERG): Electrophysiological Examination of the Retina", in *Neuro-Ophthalmology*, J. Somlai, T. Kovacs Eds., Switzerland:Springer, 2016, pp97-110.
- [6] M. Michaelides, D.M. Hunt, A.T. Moore, "The genetics of inherited macular dystrophies" , *J Med Genet*, Vol.40 No.9, 2003, pp641-650.
- [7] N Lois, G.E. Holder, C Bunce, F.W. Fitzke, A.C. Bird, "Phenotypic subtypes of Stargardt macular dystrophy-fundus flavimaculatus", *Arch Ophthalmol*, Vol.119 No.3, 2001, pp359-369.
- [8] Y Miyake, K Ichikawa, Y Shiose, Y Kawase, "Hereditary Macular Dystrophy without Visible Fundus Abnormality", *Am J Ophthalmol*, Vol.108 No.3, 1989, pp292-299.
- [9] C.J. Boon, B.J. Klevering, B.P. Leroy, C.B.Hoyng, J.E.E. Keunena, A.I.den Hollander, "The spectrum of ocular phenotypes caused by mutations in the BEST1 gene", *Prog Retin Eye Res*, Vol.28 No.3, 2009, pp187-205.
- [10] J.D. Gass, "Acute zonal occult outer retinopathy . Donders Lecture: The Netherlands Ophthalmological Society, Maastricht, Holland, June 19, 1992", *J Clin Neuroophthalmol*, No.13, 1993, pp79-97.
- [11] L.M. Jampol, P.A. Pugh et al, "Multiple evanescent white dot syndrome . 1. Clinical findings", *Arch Ophthalmol*, No.102, 1984, pp671-674.
- [12] M. Horiguchi, Y. Miyake, M. Nakamura et al, "Focal electroretinogram and visual field defect in multiple evanescent white dot syndrome", *Br J Ophthalmol*, No.77, 1993, pp452-455.
- [13] N. Suzuki, H. Yaguchi, "Research and Development on Glaucoma Diagnosis Software using a Semantic Differential Method", *KANSEI Engineering International*, Vol.6 No.4, 2007, pp47-54.
- [14] N. Suzuki, "Determination of the optimal color space from eight types of color spaces for distinguishing small retinal hemorrhages from dust artifacts", *International Journal of Biomedical Science and Engineering*, Vol.1 No.1, 2013, pp10-19.
- [15] N. Suzuki, "Distinction between Manifestations of Diabetic Retinopathy and Dust Artifacts Using Three-Dimensional HSV Color Space", *International Journal of Medical, Health, Biomedical, Bioengineering and Pharmaceutical Engineering*, Vol.10 No.3, 2016, pp153-159
- [16] C.C. Thomas, "OPTICS", Springfield, 1968, pp.156-7.